# Near-Field Pressure Measurements of Several Models in JAXA's 1m x 1m Supersonic Wind Tunnel

Yoshikazu Makino[1] and Masayoshi Noguchi[2]
*Japan Aerospace Exploration Agency, Mitaka, Tokyo 181-0015, Japan*

**Near-field pressure signatures of several simple axisymmetrical models and a 69-degree delta wing body model are measured at JAXA's 1- by 1-meter blow-down type supersonic wind tunnel in order to obtain validation data for sonic boom prediction tools. A static pressure rail which has 111 static pressure taps at 4mm interval is installed on the wind-tunnel wall. The height of the rail from the wind-tunnel wall can be changed in order to investigate the effects of the rail geometry and the shock/boundary layer interaction effects on the measured signatures.**

## Nomenclature

| | | |
|---|---|---|
| $b$ | = | wing span |
| $c$ | = | mean aerodynamic chord length |
| $C_p$ | = | pressure coefficient |
| $H$ | = | height between model and pressure rail surface |
| $H_{rail}$ | = | height of static pressure rail from wind tunnel wall |
| $L$ | = | model reference length |
| $M$ | = | Mach number |
| $p_s$ | = | static pressure |
| $p_0$ | = | total pressure |
| $Q$ | = | dynamic pressure |
| $Re_u$ | = | unit Reynolds number |
| $S_{ref}$ | = | reference area |
| $W_{rail}$ | = | width of static pressure rail |
| $X$ | = | x coordinate |
| $\alpha$ | = | angle-of-attack |
| $\beta$ | = | $\sqrt{M^2-1}$ |
| $\delta$ | = | boundary layer thickness |
| $\phi$ | = | roll angle |

## I. Introduction

JAPAN Aerospace eXploration Agency(JAXA) has been promoting the Silent Super-Sonic(S-cube) research program since 2006 for future supersonic airliners with economically viable and environmentally friendly characteristics. In this program, the flight test project named D-SEND(Drop test for Simplified Evaluation of Non-symmetrically Distributed sonic boom) is planned in order to demonstrate the advanced low-boom design concepts. In the first phase of the project(D-SEND#1), two drop tests have already been conducted at Sweden in 2011 and two scaled low-sonic-boom airplanes are designed and built for the second phase of the project(D-SEND#2)[1,2,3]. Since low-sonic-boom design validation is necessary for development of such a concept demonstrator, several near-field pressure measurement techniques in wind-tunnels have been developed at JAXA[4,5].

In this paper, a supersonic wind-tunnel test for measuring the near-field pressure signatures of several axisymmetrical models and a 69-degree swept-back angle delta wing body model are summarized. The data obtained in this test can be utilized to validate some sonic-boom prediction tools.

[1] Senior Researcher, Supersonic Transport Team, AIAA Senior Member.
[2] Associate Senior Researcher, Supersonic Transport Team.

## II. Wind Tunnel Test

### A. Facility Description

The JAXA 1- by 1-meter supersonic wind tunnel (JSWT) is a blow-down type wind tunnel where Mach number from 1.4 to 4.0 can be tested. The facility illustration is shown in Figure 1. It utilizes two high pressure dry air tanks whose maximum pressure is 2MPa and the total pressure at stagnation tank can be controlled from 150kPa to 1270kPa for each Mach number. Typical test conditions are shown in Table 1. JSWT has 1.8m-long 1m-square cross section test section. The side walls of the test section are parallel while the top and bottom walls have 5/1000 slope considering the displacement thickness of the wall boundary layer. Each side wall has a round window whose diameter is 650mm for Schlieren visualization. The bottom wall has a 560mm-diameter round plate which is utilized to install a static pressure rail in this study. The duration time of one blow is up to about 40 seconds and a typical interval between each blow is about 30 minutes. Models are supported with a strut-type sting pod whose pitch and roll angle can be controlled during blow.

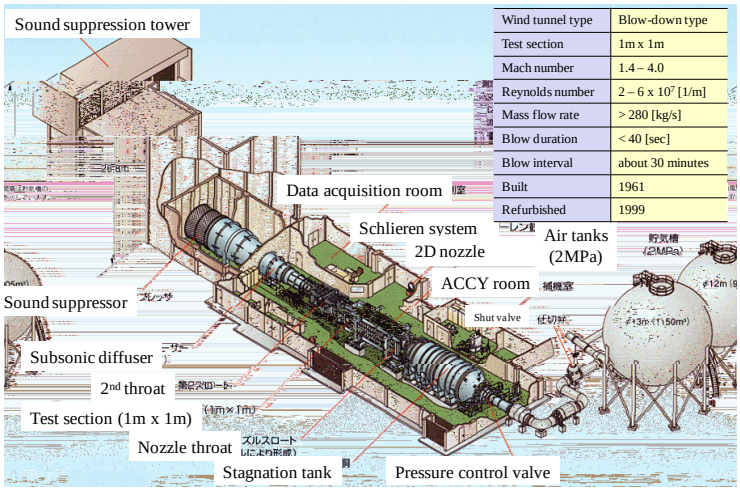


**Figure 1. Facility illustration of the 1- by 1-meter supersonic wind tunnel at JAXA.**

**Table 1. Typical test conditions.**

| Mach number $M$ | Total pressure $p_0$ [kPa] | Dynamic pressure $Q$ [kPa] | Static pressure $p_s$ [kPa] | Unit Reynolds number $Re_u$ [1x10$^6$/m] |
|---|---|---|---|---|
| 1.4 | 150 | 65 | 48 | 23 |
| 1.68 | 170 | 71 | 36 | 25 |
| 1.7 | 180 | 74 | 37 | 26 |
| 2.0 | 220 | 79 | 28 | 28 |

### B. Measurement System

A static pressure rail which has 111 static pressure taps on its surface at 4mm interval (measurement range of 440mm) is installed on the wind tunnel bottom wall. Two 15psi-range 64-port modules of the ZOC system are used for all the pressure taps. The ambient pressure is used as the back pressure of the modules. The pressure data is obtained at every 0.5sec interval with each 0.32sec data averaging. The height of the pressure rail from the wind tunnel wall can be changed from $H_{rail}$=0mm (i.e. flush mounted to wind-tunnel wall) to $H_{rail}$=52mm in order to investigate the effects of the rail geometry and the shock/boundary layer interaction on measured near-field pressure signatures. The pressure rail installation with its height of 32mm is shown in Figure 2. The rail width is $W_{rail}$=20mm as shown in the figure and a pair of square rod (length about 500mm) whose cross section has 12mm square may be attached to the side of the rail to change the rail width to $W_{rail}$=44mm. An 8-degree wedge is attached at the nose of the rail when the rail height it not $H_{rail}$=0mm.

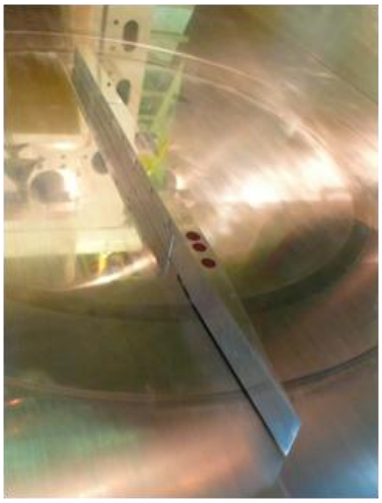

**Figure 2. Static pressure rail. ($H_{rail}$=32mm, $W_{rail}$=20mm setting)**

## C. Wind Tunnel Models

Several simple axisymmetrical models as shown in Figure 3 are used in this study. Three types of axisymmetrical model; a 6.48-degree cone, a parabolic body and a quartic body are selected. They are the same geometry used in Reference 6 in which the each geometry are referred as "the model No.1", "No.4" and "No.5", respectively. Two different sized models of $L$=80mm and $L$=160mm are built for each three geometry in order to investigate the effects of the model size on the measured pressure signatures.

A 69-degree swept-back-angle delta wing body model as shown in Figure 4 is used in this study, too. This configuration is the same as used in Reference 7 in which the model is referred as "the model No.4". The model wing span is $b$=69mm and mean aerodynamic chord $c$=64mm. The airfoil is a diamond wing with 5% thickness to chord length. The wing reference area is $S_{ref}$=3312mm$^2$. While the model in the original reference is supported with a internal balance, the model used in this study has a straight cylinder body attached to the wind tunnel sting pod.

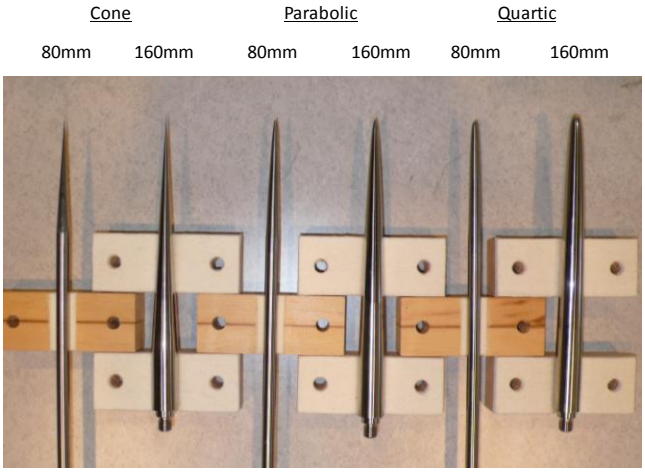


**Figure 3. Axisymmetrical models.**

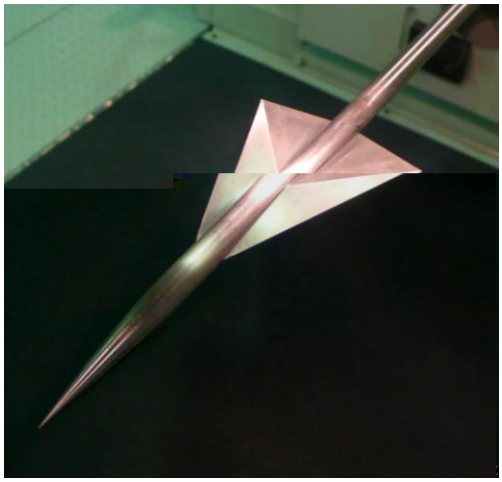

**Figure 4. 69-degree swept-back-angle delta wing body model.**

## D. Data Reduction

Any wind tunnel has its own pressure distributions on the walls in flow direction. Figure 5 shows pressure distributions in JSWT measured by the static pressure rail with different rail heights. It shows that the JSWT has its own pressure distribution even in the case of $H_{rail}$=0mm. The pressure variation gets larger as the rail height increases because the rail itself generates the pressure disturbances in the free stream.

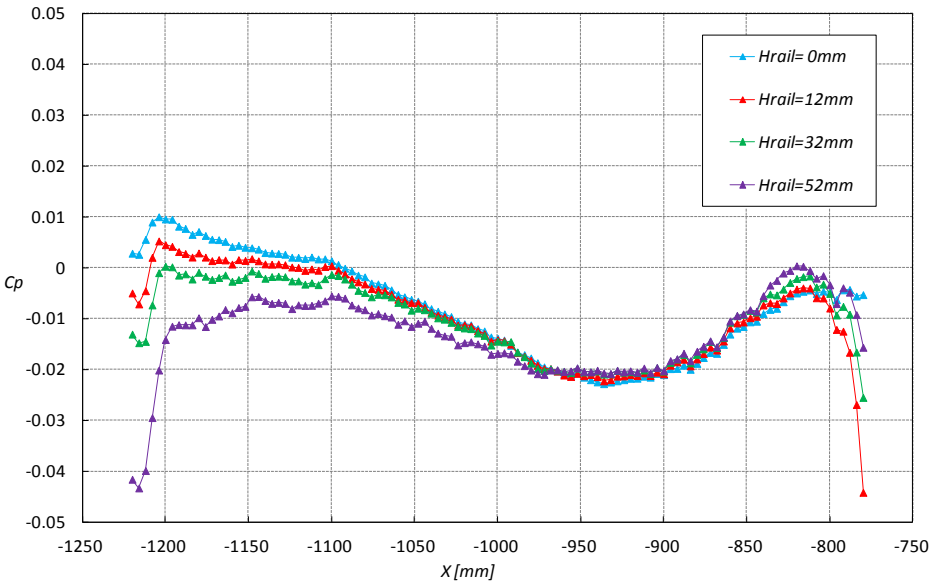


**Figure 5. Pressure distributions without models.($M$=1.4, $W_{rail}$=20mm)**

Therefore the pressure waves generated from the models should be obtained by subtracting the pressure without the models from the data with the models. Figure 6(a) and 6(b) show typical results of this data correction for the parabolic axisymmetrical model and the 69-degree delta wing body model, respectively. The result that *Cp* differences at front part of the signatures are almost zero shows the model on/off correction works well in the test. Although some pressure ports show different pressure value from the neighboring ports such as at the port about X=-980mm at M=1.68 shown in Figure 6(b) which may be caused by a local protuberance around the port on the pressure rail surface, they usually work well with the model on/off correction if the local disturbances affect similarly in both model on and off cases.

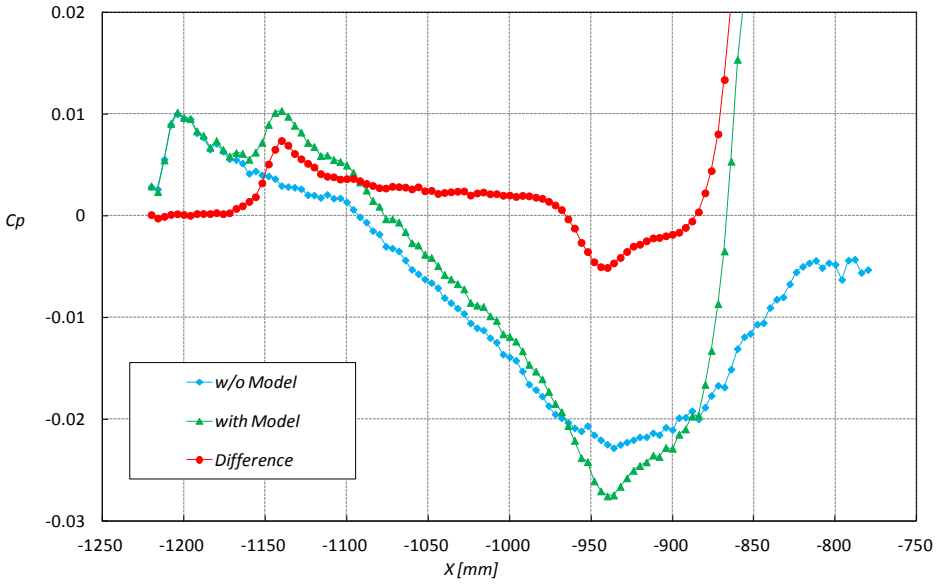


(a) Parabolic model, $M$=1.4, $\alpha$=0deg, $H_{rail}$=0mm, $W_{rail}$=20mm

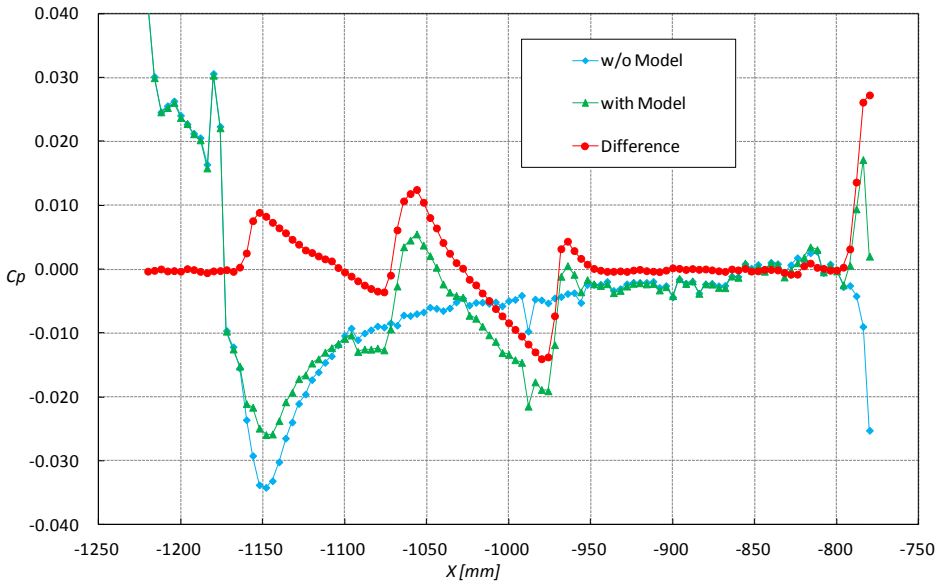


(b) 69-degree delta wing body model, $M$=1.68, $\alpha$=0deg, $H_{rail}$=12mm, $W_{rail}$=44mm

**Figure 6. Model on/off correction.**

## III. Results and Discussion

### A. Measurement Accuracy

Figure 7(a) and 7(b) show the *Cp* variations during the blows withouu20(e)4( )d4(as)9h.52 674.78 Tm[( )] TJ443.1BT1 0 0 1



Cp

## B. Rail Height Effects on Axisymmetrical Models

In order to investigate the effects of the rail height on the measured signature, the near-field pressure signatures of three types of the axisymmetrical model(cone, parabolic, and quartic) are measured using the rail with 4 different rail heights($H_{rail}$=0mm, 12mm, 32mm, and 52mm). Figure 8,9, and 10 show the measured signatures for the cone, the parabolic, and the quartic model, respectively. Two different model sizes, $L$=80mm and $L$=160mm, are used for each geometry. The horizontal axis of the graph is the distance nondimensionalized by the model length from the point where the Mach line from the model nose hits the rail surface. The near-field pressure signatures of the $L$=80mm cone model shown in Figure 8(a) show some effects of the rail height on the signatures. The measured signature moves backwards as the rail height increases. The pressure signature measured with higher rail height tends to show some small pressure variations in the middle of the signature which are not shown in the signature measured with rail height of $H_{rail}$=0mm. Compared to these signatures of the $L$=80mm model, the measurement resolution (number of measurement points in the model length) of the signatures of $L$=160mm model shown in

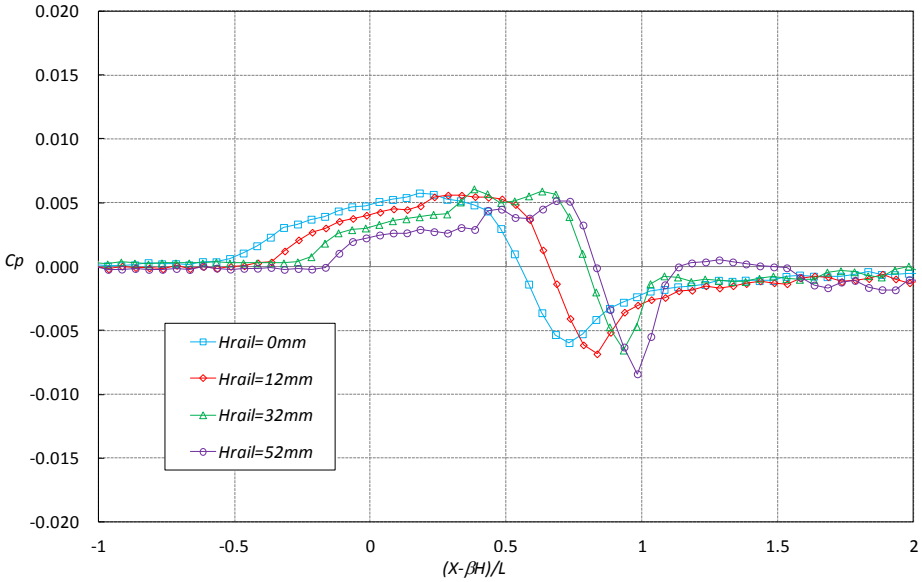


(a) $L$=80mm

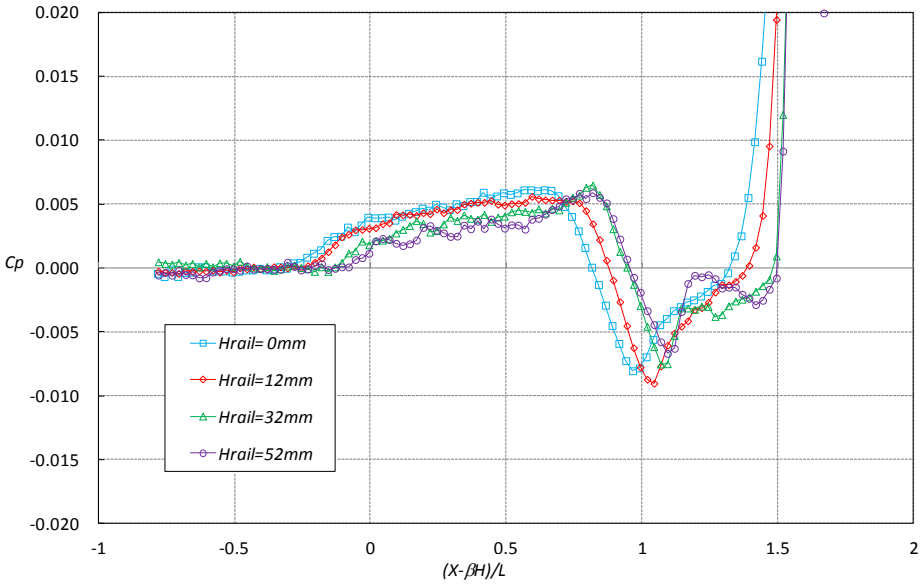


(b) $L$=160mm

**Figure 8. Rail height effects on measured pressure signatures. (Axisymmetrical Cone model, $M$=1.4, $\alpha$=0deg, $H/L$=5.0, $W_{rail}$=20mm)**

Figure 8(b) becomes twice with the same pressure rail. Although the rail height effects on the measured signatures are similar to those on the $L$=80mm model results, the backward shift of the signature due to the rail height increase are smaller than the previous case in nondimensionalized distance. This suggests that the shift does not depend on the model size but on the rail height. If the shock wave from the model nose reflects at a certain vertical distance from the wind tunnel wall in the boundary layer out of relation to the rail height, the position of the measured nose shock moves backwards in proportion as the rail and model moves upwards because the vertical pressure gradient in the boundary layer is presumed to be zero. Although the pressure signature of the $L$=160mm model measured with higher rail height also tends to show some small pressure variations in the middle of the signature, these variations are different from those in the $L$=80mm model results as typically shown in the aft part of the signature around $(X-\beta H)/L$=1.0. This fact suggests that the effects of the rail height on the measured signature depend on both model and pressure rail.

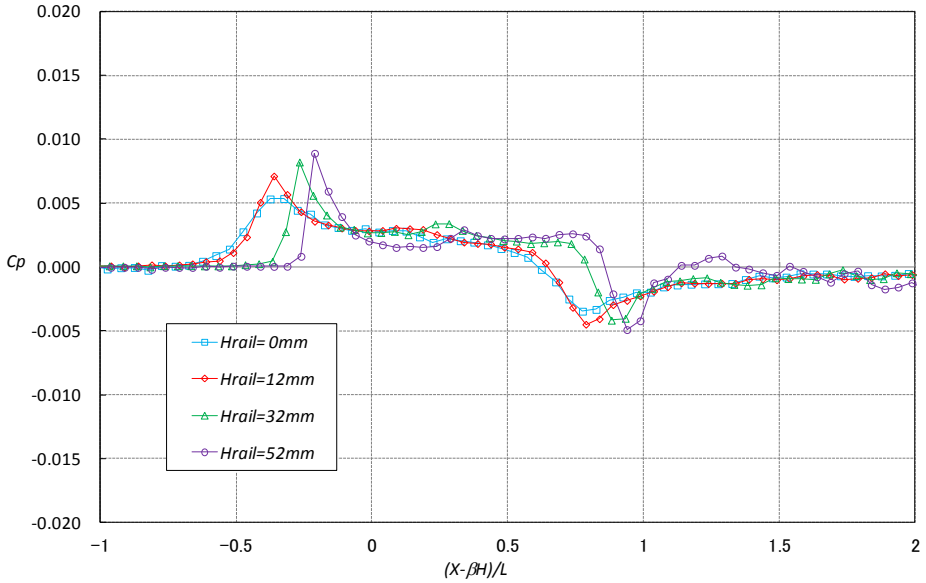


(a) $L$=80mm

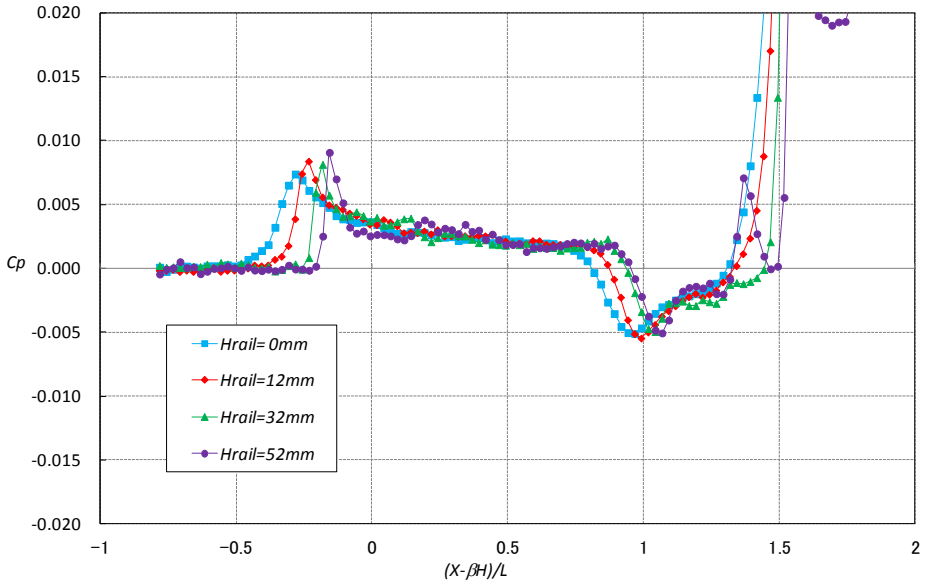


(b) $L$=160mm

**Figure 9. Rail height effects on measured pressure signatures. (Axisymmetrical parabolic model, $M$=1.4, $\alpha$=0deg, $H/L$=5.0, $W_{rail}$=20mm)**

The similar tendency of the signature shift and additional small pressure variations are shown in the measured signatures of the parabolic and the quartic model in Figure 9 and 10, respectively. Since the noses of these models are blunt compared to the cone model and hence the nose shocks generate sharper pressure peaks, the pressure peaks clearly show the effects of shock wave/boundary layer interaction. The nose pressure peak measured with the rail height of $H_{rail}$=0mm gets smaller and dampened due to strong shock/boundary layer interaction while the pressure signatures measured with the higher rails show the small pressure variations due to the shock/rail interaction. In Reference 8, the boundary layer profiles of JSWT are measured using a Pitot rake. The boundary layer thickness is about $\delta$=48mm for $M$=1.4 and $\delta$=53mm for $M$=2.0. Since the velocity profile in the boundary layer of JSWT agrees well with the 1/7$^{th}$ power law shape, the displacement thickness is estimated less than 10mm. Considering the pressure rail above the displacement thickness of the boundary layer is presumed to affect the free-stream and interfere with the shock waves from the model, the rail height should be 10mm or lower. Therefore the rail height of $H_{rail}$=12mm in this study seems to be a moderate compromise for both shock/boundary layer and shock/rail interference effects.

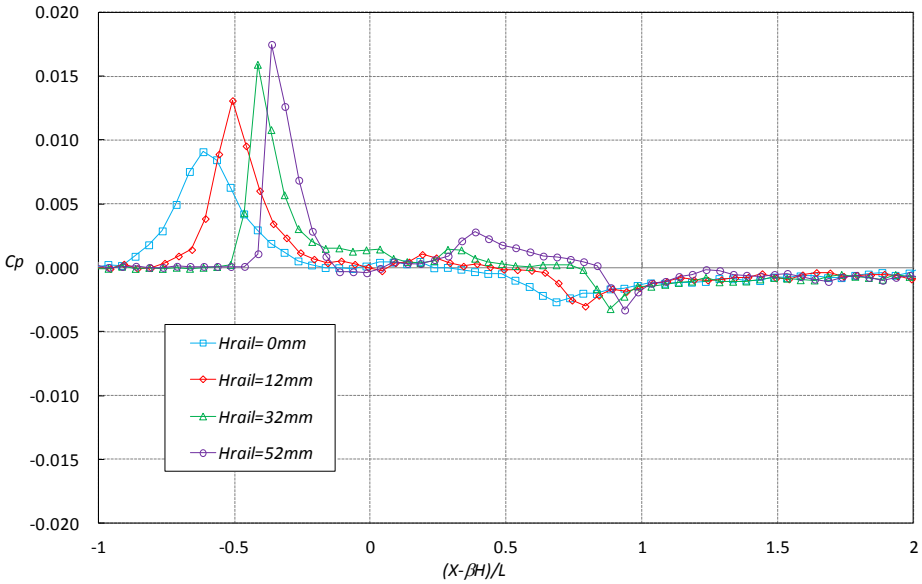


(a) $L$=80mm

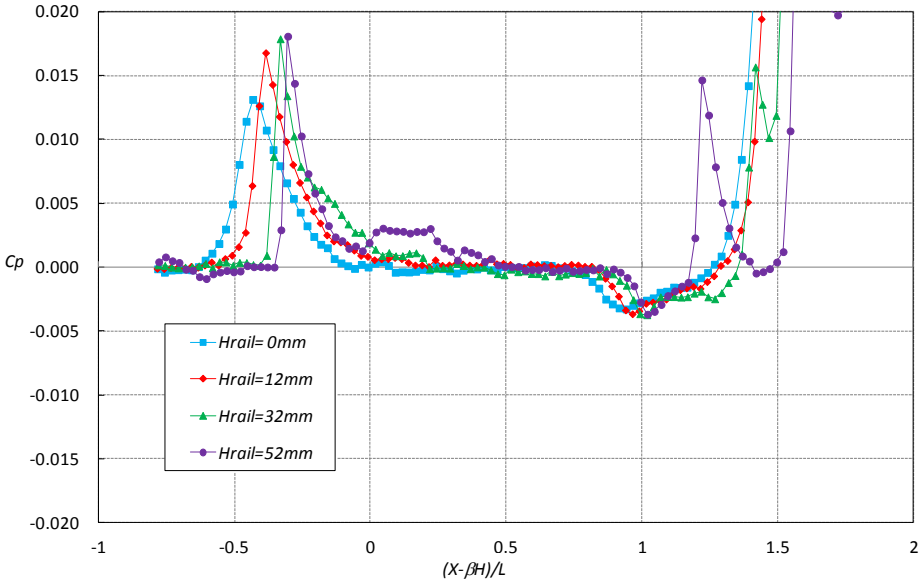


(b) $L$=160mm

**Figure 10. Rail height effects on measured pressure signatures. (Axisymmetrical quartic model, $M$=1.4, $\alpha$=0deg, $H/L$=5.0, $W_{rail}$=20mm)**

### C. 69-degree Delta Wing Body Model

Figure 11 shows the repeatability of the near-field pressure measurement for the 69-degree swept-back-angle delta wing body model at angle-of-attack of 0 degree. Two consecutive blows (Run number #28119 and #28120) are conducted in which the pressure data is acquired 4 times during 2 seconds for each blow. All the data shown in the graph use the same "Model off" data which is the average of the pressure data obtained without the model(Run number #28118). The data fluctuation is almost within 0.0005 in Cp which means that the pressure measurement accuracy through different runs is about the same level as that in single blow shown in Figure 7(b).

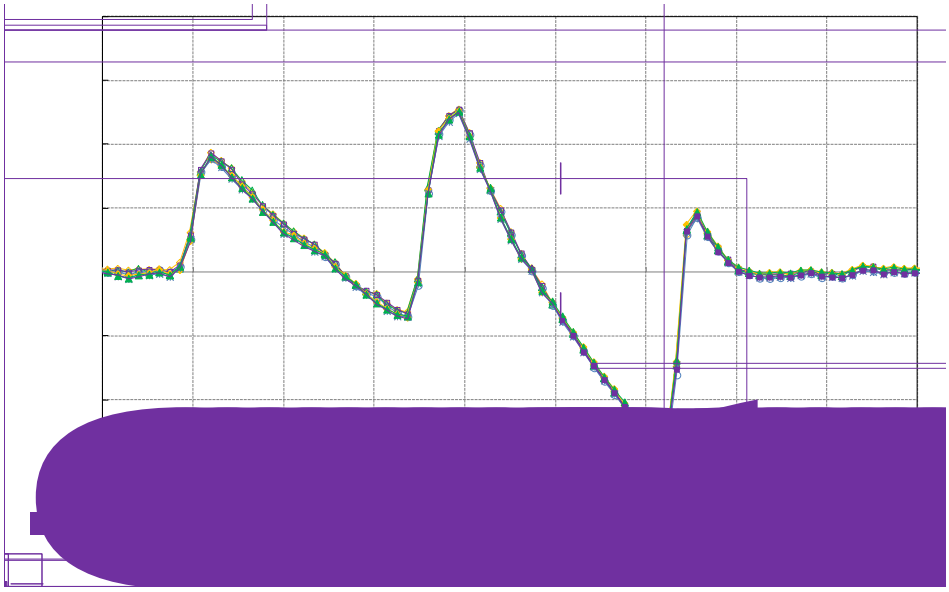

**Figure 11. Measured pressure signatures of 69-degree delta wing body model. ($M$=1.68, $\alpha$=0deg, $\phi$=0deg, $H/L$=3.6, $H_{rail}$=12mm, $W_{rail}$=44mm)**

Figure 12 shows the pressure signatures of the delta wing body model with different roll angles. The test conditions are at Mach number of $M$=1.68 and the model angle-of-attack of $\alpha$=0deg and the height to model length ratio of $H/L$=3.6 which are the same conditions in Reference 7.

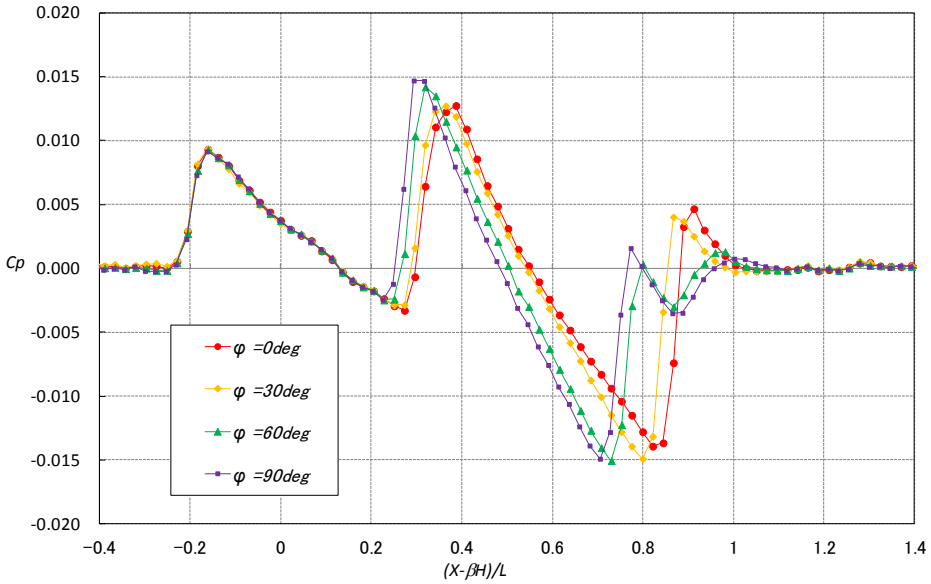


**Figure 12. Measured pressure signatures of 69-degree delta wing body model for different roll angles. ($M$=1.68, $\alpha$=0deg, $H/L$=3.6, $H_{rail}$=12mm, $W_{rail}$=44mm)**

## IV. Summary

Near-field pressure signatures of several simple axisymmetrical models and a 69-degree delta wing body model are measured at JAXA's 1- by 1-meter blow-down type supersonic wind tunnel(JSWT) in order to obtain validation data for sonic boom prediction tools.

1) The near-field pressure measurement accuracy at JSWT using the pressure rail is within 0.0008 in *Cp* at *M*=1.4 and within 0.0005 in *Cp* at *M*=1.68.
2) The model on/off correction works well to obtain a near-field pressure signature of a model.
3) The shock/boundary layer interaction dampens the measured pressure peaks heavily when the rail height is $H_{rail}$=12mm or lower.
4) The shock/rail interaction introduces some additional pressure variations in the measured signatures apparently when the rail height is $H_{rail}$=32mm or higher.
5) The near-field pressure signatures of the 69-degree delta wing body model at angle-of-attack of 0 degree which seems to be appropriate for qualitative tool validation are obtained.

## Acknowledgments

The authors express their sincere gratitude to the JSWT staffs for their support in the wind-tunnel test and to Mr.Mitsunori Watanabe for his provision of the boundary layer profile information of the JSWT.

## References

[1]Honda, M. and Yoshida, K., "D-SEND project for low sonic boom design technology," *Proceedings of the 28th Congress of the International Council of the Aeronautical Sciences*, ICAS 2012-1.2.1, 2012.

[2]Naka, Y., "Sonic boom data from D-SEND#1," *JAXA Research Memorandum*, JAXA-RM-11-010E, 2012.

[3]D-SEND Database, URL: http://d-send.jaxa.jp/d_send_e/index.html [cited 30 May 2012].

[4]Makino, Y., Suzuki, K., Noguchi, M. and Yoshida, K., "Nonaxisymmetrical fuselage shape modification for drag reduction of low-sonic-boom airplane," *AIAA Journal*, Vol.41, No.8, 2003, pp.1413-1420.

[5]Furukawa, T., Makino, Y., Noguchi, M. and Ito, T., "Supporting system study of wind-tunnel models for validation of aft-sonic-boom shaping design," *26th AIAA Applied Aerodynamics Conference*, AIAA 2008-6596, 2008.

[6]Carlson, H.W., Mack, R.J. and Morris, O.A., "A wind-tunnel investigation of the effect of body shape on sonic-boom pressure distributions," *NASA Technical Note*, NASA TN D-3160, 1965.

[7]Hunton, L.W., Hicks, R.M. and Mendoza, J.P., "Some effects of wing planform on sonic boom," *NASA Technical Note*, NASA TN D-7160, 1973.

[8]Watanabe, M., Iijima, H., Sato, M., Nagai, S., and Nomura, R., "Measurement of the boundary layer profiles in the test section of the 1m x 1m supersonic wind tunnel," *JAXA Research Memorandum*, JAXA-RM-08-011, 2009.